

⁷⁹Br Nuclear Quadrupole Relaxation in the High Temperature Modification of Niobium Pentabromide

Noriaki Okubo, Harutaka Sekiya *, Chiaki Ishikawa **, and Yoshihito Abe
Institute of Physics, University of Tsukuba, Tsukuba 305, Japan

Z. Naturforsch. **47a**, 713–720 (1992); received December 13, 1991

The spin-lattice relaxation time of ⁷⁹Br NQR has been measured between 4.2 K and room temperature. The result is compared with that of ³⁵Cl NQR in NbCl₅. The origin of the relaxation is attributed to the quadrupolar interaction and the temperature dependence is explained by the Raman process. The Debye temperature is determined to be 94 K and the relaxation time is related with the NQR frequency through the covalency.

Key words: Niobium pentabromide, Nuclear quadrupole resonance, Spin-lattice relaxation, Raman process, Debye temperature.

1. Introduction

Many transition metal pentahalides crystallize with similar structures [1] so that in these a systematic investigation of the halogen NQR is possible. Since the spin-lattice relaxation of both chlorine and bromine nuclei with spin $I = 3/2$ is characterized by one relaxation time T_1 , its value can be determined without ambiguity. However, only the spectra have been studied so far [1] while a dynamical study is missing. Recently we reported a study on the NQR relaxation of NbCl₅ [2] and showed that the Raman process is dominant in this compound. A theory of nuclear spin-lattice relaxation due to the Raman process was proposed by Kranendonk [3] for ionic crystals and later it was extended to the case involving covalent bonding [4]. These theories involve the Debye temperature, which is not known for NbCl₅. Moreover, they were developed for simple structures only; no detailed analysis was made for NbCl₅. In successively examined NbBr₅, however, a similar temperature dependence of T_1 was observed for the bromine nuclei. The present paper presents experimental results on T_1 (⁷⁹Br) in NbBr₅ and a detailed analysis, together with a comparison with T_1 (³⁵Cl) in NbCl₅.

NbCl₅ and NbBr₅ crystallize isomorphous [5]. The unit cell is monoclinic, space group C2/m. The unit cell consists of twelve molecules. For these com-

pounds, however, dimorphism had been reported [6]. As for NbBr₅, the second phase is orthorhombic and the unit cell contains eight formula units, the tentative space group being D_{2h}⁹–Pbam [7]. From comparison of the NQR spectra and the result of X-ray analysis it was clarified that in both compounds the monoclinic phase corresponds to the low temperature modification (LTM) and the orthorhombic phase of NbBr₅ to the high temperature modification (HTM) [8–11]. The structure of HTM in NbCl₅ is not determined, but from the similarity of the NQR spectrum to that of HTM of NbBr₅ the structure is considered to be close to that of HTM of NbBr₅.

In the following we refer to the HTM, unless described otherwise. In the next section the experimental details are described. The results are presented in Sect. 3, they are analyzed and discussed in Sect. 4 and the conclusion is given in Section 5.

2. Experiment

The experiment on NbBr₅ was carried out similar to that on NbCl₅ [2]. The sample was the same as used in the investigation of the ⁹³Nb and ⁷⁹Br NQR spectra [9, 11] and was identified to be orthorhombic. The temperature was controlled within 0.1 K and measured with a gold-iron vs. chromel thermocouple to an accuracy of 0.1 K.

The ⁷⁹Br NQR spectrum consists of two singlet lines (A and A') around 110 MHz and two unresolved doublet lines (BB' and CC') around 60 MHz [11]. The NQR signal was observed by a pulsed method. The

* Alps Electric Co., Izumi, Sendai, Japan.

** Anan Senior High School, Shimo-ina, Nagano, Japan.

Reprint request to Dr. N. Okubo, Institute of Physics, University of Tsukuba, Tsukuba 305, Japan.

0932-0784 / 92 / 0600-0713 \$ 01.30/0. – Please order a reprint rather than making your own copy.



Dieses Werk wurde im Jahr 2013 vom Verlag Zeitschrift für Naturforschung in Zusammenarbeit mit der Max-Planck-Gesellschaft zur Förderung der Wissenschaften e.V. digitalisiert und unter folgender Lizenz veröffentlicht: Creative Commons Namensnennung-Keine Bearbeitung 3.0 Deutschland Lizenz.

Zum 01.01.2015 ist eine Anpassung der Lizenzbedingungen (Entfall der Creative Commons Lizenzbedingung „Keine Bearbeitung“) beabsichtigt, um eine Nachnutzung auch im Rahmen zukünftiger wissenschaftlicher Nutzungsformen zu ermöglichen.

This work has been digitalized and published in 2013 by Verlag Zeitschrift für Naturforschung in cooperation with the Max Planck Society for the Advancement of Science under a Creative Commons Attribution-NoDerivs 3.0 Germany License.

On 01.01.2015 it is planned to change the License Conditions (the removal of the Creative Commons License condition “no derivative works”). This is to allow reuse in the area of future scientific usage.

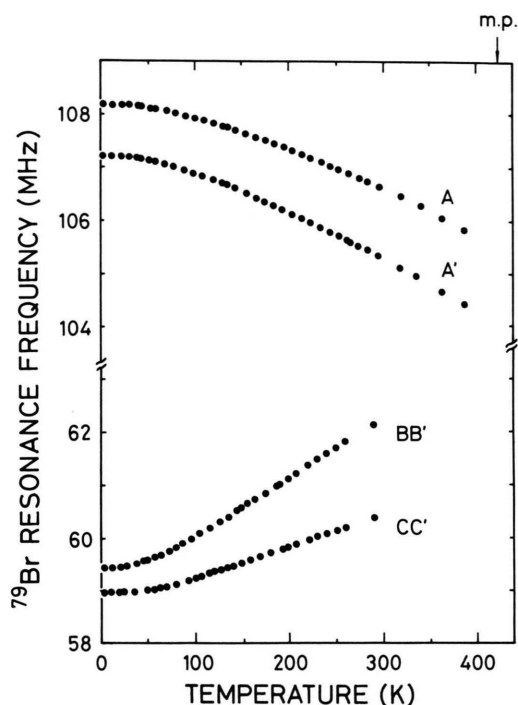


Fig. 1. Temperature dependence of the ^{79}Br NQR frequencies in HTM of NbBr_5 .

peak-to-peak amplitude of the rf field at the sample coil was estimated to be 20 G for 60 MHz and 16 G for 110 MHz. At each temperature the apparatus was tuned with the center frequency of the resonance by monitoring the spin-echo signal. Typically, at 77 K, the signal-to-noise ratio was 50 after 500 times averaging, T_2 was 250 μsec and T_2^* was 20 μsec . T_1 was determined by measuring the echo height $S(t)$ as a function of repetition time t of 90° - τ - 180° pulse sequences. For the well resolved lines A and A' respective T_1 's were measured, while for the unresolved lines BB' and CC' the T_1 's were measured with the frequency corresponding to the centers of the resonance. In particular, at 63 K and 290 K, the respective T_1 's for the component lines of the doublet ones were also measured by observing the echo height after saturation by 90° pulse trains of the corresponding frequencies, and it was confirmed that they are nearly identical to each other and to those obtained by the former method.

3. Results

The temperature dependence of the ^{79}Br NQR frequencies in NbBr_5 is shown in Figure 1. The separa-

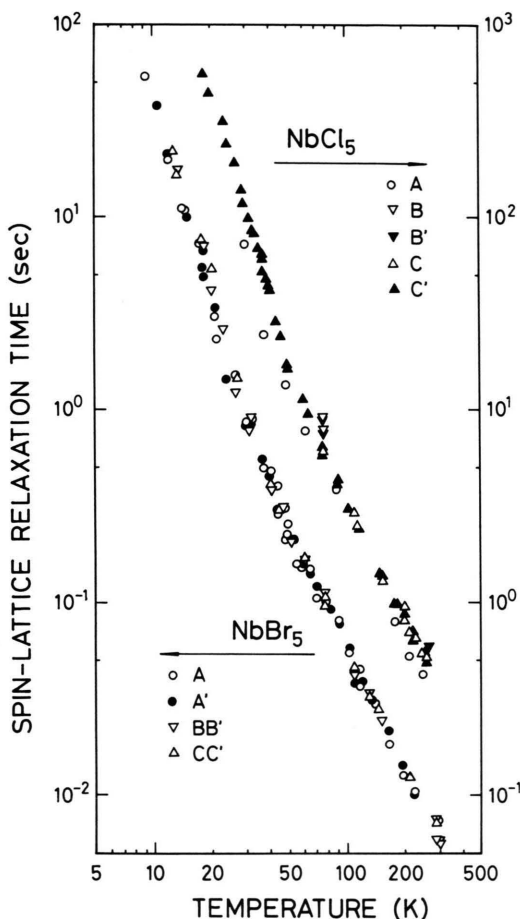


Fig. 2. Temperature dependence of the relaxation times of ^{35}Cl and ^{79}Br in HTM of NbCl_5 and NbBr_5 . The data for NbCl_5 are from [2] with addition of some points for the A, B, and B' lines.

tion of the components of the doublet lines is small ($\lesssim 120$ kHz), so that the averaged frequencies are shown. The temperature dependence of the T_1 's for the ^{79}Br NQR lines is shown in Fig. 2, together with that for ^{35}Cl lines in NbCl_5 [2]. In NbBr_5 , the values of T_1 for each line are nearly equal within experimental errors.

In NbCl_5 , non-single exponential recovery and a suppression of T_1 were earlier observed at low temperatures. Since these phenomena disappeared after annealing, they were attributed to impurities (oxides). In the figure the data after annealing are shown. In case of NbBr_5 the sample was annealed and the observed recovery curves were single-exponential at all measured temperatures. T_1 increased up to 2400 sec for A, 1900 sec for A', 2400 sec for BB' and 1700 sec for CC'

at 4.2 K. Moreover, at given temperatures the values are much smaller than those for NbCl_5 . Therefore the data of NbBr_5 may be regarded as free from impurity effects down to low temperatures.

The ratio $T_1(^{79}\text{Br})^{-1}/T_1(^{81}\text{Br})^{-1}$ was 1.2 ± 0.3 for all lines at 77 K and 290 K. This is close to the squared ratio of the nuclear quadrupole moments Q , $[Q(^{79}\text{Br})/Q(^{81}\text{Br})]^2 = (0.31/0.26)^2 = 1.42$ rather than that of the magnetic moments μ , $[\mu(^{79}\text{Br})/\mu(^{81}\text{Br})]^2 = (2.11/2.27)^2 = 0.86$. Therefore the relaxation in this system is considered to originate mainly from the quadrupolar interaction.

At temperatures higher than 50 K the temperature dependence of T_1 is approximately proportional to T^{-2} , and at lower temperatures to T^{-4} . This temperature dependence fairly resembles that in NbCl_5 . It is worthwhile noting that, on the log-log plot of Fig. 2, the curves for NbBr_5 can be superposed on those for NbCl_5 by a translation, indicating that they may be described by a common equation if properly scaled.

4. Discussion

In the monoclinic phase of NbCl_5 and NbBr_5 the halogen atoms form a slightly distorted octahedron involving one niobium atom at the center, as shown in Figure 3. Two octahedra share one common edge to form a dimer, so that there are three kinds of positions for the halogen atoms: bridging, equatorial and axial. The dimeric structure is expected to be retained in HTM of both compounds [1]. Therefore it is reasonable to assign lines A and A' to bridging, BB' to equatorial and CC' to axial halogen nuclei, as done for NbCl_5 [1, 11].

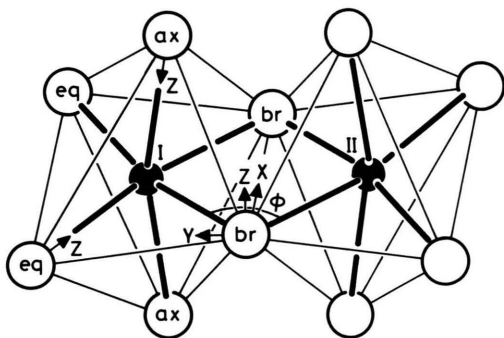


Fig. 3. Dimeric structure of NbCl_5 and NbBr_5 [5]. The symbols ax, eq and br mean axial, equatorial and bridging, respectively. The arrows represent the principal z axes of the EFG. For bridging nuclei the z axis is normal to the equatorial plane and the x axis is directed toward another bridging atom.

For the quadrupolar relaxation in non-metallic substances three mechanisms have been considered successfully [12]: torsional oscillations, reorientation of atomic groups and the Raman process due to lattice vibrations. In contrast to the former two mechanisms, the third one predicts for T_1 a temperature dependence close to the observed one. Therefore in the following the Raman process alone is assumed.

4.1 Relaxation due to Raman Process

In the quadrupole relaxation due to the first-order Raman process, the change of nuclear spin direction is associated with simultaneous absorption of one phonon and emission of another phonon, with adequate energies. A detailed calculation of the transition probability was made for NaCl-type ionic crystals on the basis of a point-charge model, and the importance of the covalency effect was demonstrated as well as the shielding and anti-shielding effects [3]. The theory was applied to Cu_2O [12, 13], and a possibility for determining the Debye temperature was pointed out [13].

Yosida and Moriya [4] showed from an order estimation that, when even a small degree of covalency exists, the probability due to ionicity can be neglected, and they calculated on the basis of covalency the transition probability due to the Raman process for NaCl- and CsCl-type structures. Their result may be applied to transition metal halides with some modifications, because they possess a certain degree of covalency [1]. However, the applicability to the present structure is not necessarily obvious because it is assumed in their calculation that all the ions are equivalent concerning the lattice vibrations (cf. [4], p. 43, 1.1; [3], p. 78, 1.6). This point is discussed later.

According to them, T_1^{-1} for $I = 3/2$ is given by

$$T^{-1} = \frac{3e^4 Q^2 \langle r^{-3} \rangle_H^2 c^3}{100\pi^3 a^7 d^2 v^3} T^{*2} \sum_{v=1}^4 (N_{1v} + 4N_{2v}) D_v(T^*), \quad (1)$$

where a denotes the equilibrium distance from the halogen ion to the metal ion, d the density of the crystal, v the sound velocity, and T^* the temperature reduced by the Debye temperature θ . $\langle r^{-3} \rangle_H$ represents the expectation value with respect to valence p electrons of halogen ions (cf. [4], p. 41). c is defined as $c = k_m a$ with $k_m = (6\pi^2 N/V)^{1/3}$, N being the number of atoms in the unit cell of volume V . v is related with θ by

$$\hbar \omega_m = \hbar v k_m = \kappa \theta, \quad (2)$$

where κ is the Boltzmann constant.

With a measure of covalency, λ , and its first and second derivatives with respect to the interionic distance, λ' and λ'' , $N_{\mu\nu}$ ($\mu=1, 2$) for the present structure is expressed as follows: For terminal (axial and equatorial) atoms

$$\begin{aligned} N_{11} &= N_{12} = 4\lambda^2 \left(1 - \frac{a\lambda'}{\lambda}\right)^2, \\ N_{13} &= N_{14} = 0, \\ N_{21} &= N_{22} = \lambda^2, \\ N_{23} &= N_{24} = 0, \end{aligned} \quad (3)$$

and for bridging atoms

$$\begin{aligned} N_{11} &= N_{12} = 8\lambda^2 \left[1 - \frac{a\lambda'}{\lambda} + \frac{1}{2} \left(\frac{a\lambda'}{\lambda}\right)^2\right], \\ N_{13} &= N_{14} = 8\lambda^2 \left[(-1 + 2\cos^2\phi) + \left(\frac{a\lambda'}{\lambda}\right) \cdot (1 - 2\cos^2\phi) + \frac{1}{2} \left(\frac{a\lambda'}{\lambda}\right)^2 \cos^2\phi\right], \\ N_{21} &= N_{22} = \lambda^2 \left[\frac{7}{2} - \frac{7}{2} \left(\frac{a\lambda'}{\lambda}\right) + \frac{5}{4} \left(\frac{a\lambda'}{\lambda}\right)^2 + \frac{1}{8} \left(\frac{a^2\lambda''}{\lambda}\right)^2\right], \\ N_{23} &= N_{24} = \lambda^2 \left[\left(\frac{1}{2} - 13\cos^2\phi + 16\cos^4\phi\right) + \left(\frac{a\lambda'}{\lambda}\right) \left(-\frac{3}{2} + 18\cos^2\phi - 20\cos^4\phi\right) + \left(\frac{a\lambda'}{\lambda}\right)^2 \left(\frac{7}{8} - \frac{47}{8}\cos^2\phi + \frac{25}{4}\cos^4\phi\right) + \left(\frac{a^2\lambda''}{\lambda}\right) (1 - 5\cos^2\phi + 4\cos^4\phi) + \left(\frac{a\lambda'}{\lambda}\right) \left(\frac{a^2\lambda''}{\lambda}\right) \left(-\frac{1}{4} + \frac{11}{4}\cos^2\phi - \frac{5}{2}\cos^4\phi\right) + \left(\frac{a^2\lambda''}{\lambda}\right)^2 \left(-\frac{1}{8}\cos^2\phi + \frac{1}{4}\cos^4\phi\right)\right], \end{aligned} \quad (4)$$

where ϕ denotes the angle which the two bridging bonds make, as shown in Figure 3.

The structure-dependent function $D_v(T^*)$ is defined by

$$D_v(T^*) = T^* \int_0^{1/T^*} \frac{x^2 e^x}{(e^x - 1)^2} L_v(c T^* x) dx, \quad (5)$$

where $x = \hbar\omega/\kappa T$ and

$$\begin{aligned} L_1(ka) &= \{S_1^2\}_{\mathbf{k}}^2 = \left\{\frac{1}{2} - \frac{1}{2}f(2ka)\right\}^2, \\ L_2(ka) &= \{C_1^2\}_{\mathbf{k}}^2 = \left\{\frac{3}{2} - 2f(ka) + \frac{1}{2}f(2ka)\right\}^2, \\ L_3(ka) &= \{S_1 S_2\}_{\mathbf{k}}^2 = \left\{-\frac{1}{2}f(\sqrt{2(1+\cos\phi)}ka) + \frac{1}{2}f(\sqrt{2(1-\cos\phi)}ka)\right\}^2, \\ L_4(ka) &= \{C_1 C_2\}_{\mathbf{k}}^2 \\ &= \left\{1 - 2f(ka) + \frac{1}{2}f(\sqrt{2(1+\cos\phi)}ka) + \frac{1}{2}f(\sqrt{2(1-\cos\phi)}ka)\right\}^2, \end{aligned} \quad (6)$$

where

$$S_n = \sin(a\mathbf{k} \cdot \mathbf{n}), \quad C_n = \cos(a\mathbf{k} \cdot \mathbf{n}) - 1, \quad f(y) = \frac{\sin y}{y}, \quad (7)$$

and $\{\}_{\mathbf{k}}$ means the average about the direction of \mathbf{k} , \mathbf{k} being the wave vector of the phonon, \mathbf{n} the unit vector from halogen to metal ion. These expressions are derived in the Appendix.

At $T^* > 1$, $D_v(T^*)$ is nearly constant, but for $T^* < 1$ it decreases rapidly toward zero at $T^* = 0$. Thus, in (1), $D_v(T^*)$ characterizes the behavior of T_1^{-1} deviating from the T^2 dependence with lowering temperature.

4.2 Estimation of Debye Temperature

The Debye temperature θ is not known for NbCl_5 and NbBr_5 . However, if the observed temperature dependence of T_1 can be explained by the Raman process, the values may be estimated by an appropriate fitting. By the use of the definitions in [4], $N_{\mu 1} = N_{\mu 2}$ and $N_{\mu 3} = N_{\mu 4}$ ($\mu=1, 2$), (1) can be rewritten as

$$(T_1 T^2)^{-1} = (\tau \theta^2)^{-1} [\{D_1(T^*) + D_2(T^*)\} + n \{D_3(T^*) + D_4(T^*)\}], \quad (8)$$

where

$$\tau^{-1} = \frac{3e^4 Q^2 \langle r^{-3} \rangle_{\text{H}}^2 c^3}{100\pi^3 a^7 d^2 v^3} (N_{11} + 4N_{21}) \quad (9)$$

and

$$n = \frac{N_{13} + 4N_{23}}{N_{11} + 4N_{21}}. \quad (10)$$

As seen in (3) and (4), only for the bridging atoms n takes a nonvanishing value which depends on a , λ'/λ , and λ''/λ but not on λ itself.

The crystal data used to evaluate (5) are listed in Table 1. The values for NbCl_5 are those determined by the X-ray analysis for the LTM, but they may be used also for the HTM whose structure is not known be-

Table 1. Used crystal data and halogen coupling constants.

Compound	NbCl_5	NbBr_5
N	72	48
$V(\text{\AA}^3)$	1935	1472
$a(\text{\AA})$ {axial	2.302	2.374
equatorial	2.250	2.374
bridging	2.555	2.734
ϕ (degree)	101.3	101.3
$d(\text{g/cm}^3)$	2.78	4.44
$e^2 Q q_{\text{at}}/h(\text{MHz})$	109.74	769.756

cause structural similarity is strongly suggested by the NQR spectra. On the other hand, for NbBr_5 , N and V are determined for both phases and the values in the table are those for the HTM, but the atomic positions, whence the a 's, are not determined for either phase. So they were estimated from the ionic and covalent distances with the ionicity calculated empirically from the electronegativities [14]. For the covalent distance, the bond characters determined from the bromine NQR frequencies were taken into account [1]. A similar procedure for LTM of NbCl_5 yields values for a equal, within 0.05%, to those in the table. This justifies the estimation of a for NbBr_5 . For ϕ in NbBr_5 the same value as in NbCl_5 was used. It can be shown numerically that practically no error arises from this replacement. On the other hand, the difference of N/V between the two phases of NbBr_5 is smaller than 3% [5, 7] and hence that of k_m is not greater than 1%. Therefore in NbCl_5 the use of the values of N/V for the LTM in place of that for the HTM is also justified.

The integration in (5), performed numerically, was made for each halogen position with the corresponding value of $c = k_m a$. Although the above expressions are derived on the basis of the equivalency of the ions, the fitting can be made for each line with assumption of the respective values for θ as well as for τ . Then, by a least-squares-fitting of (8) for the axial lines C' in NbCl_5 and CC' in NbBr_5 values of 146 K and 95 K were obtained for the respective θ . The results are shown in Figure 4. Also for the other lines in NbBr_5 similar fittings were made and close values were obtained. In Table 2 the result for the fitting with a common θ for four lines are shown. On the other hand, for other lines than C' in NbCl_5 , the data of T_1 in Fig. 2 are not sufficient, so that the value 146 K for the C' line was used as a common θ . By (2) the corresponding values of v are 1.47 for NbCl_5 and 0.99 for NbBr_5 in units of 10^5 cm/sec . Since the values of τ are not significantly different within each position in either com-

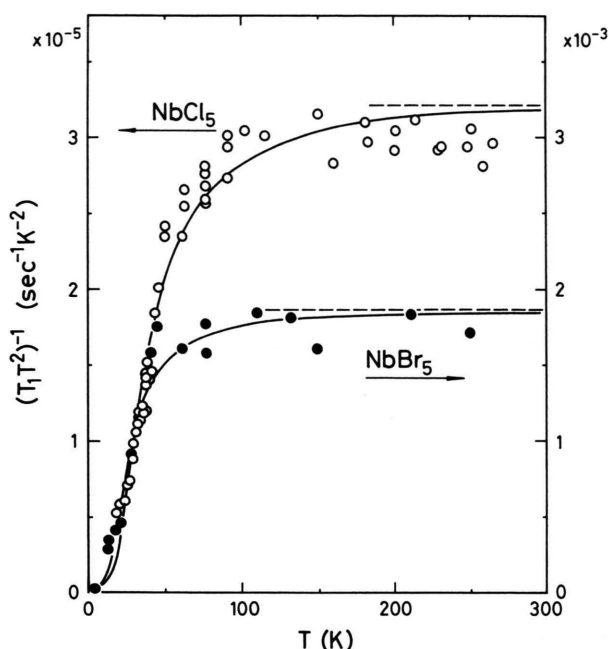


Fig. 4. A least-squares-fitting of (8) for the axial line in NbCl_5 and NbBr_5 . The solid lines represent the theoretical curves for $\theta = 146 \text{ K}$ and $\tau = 0.77 \text{ sec}$ in NbCl_5 and for $\theta = 95 \text{ K}$ and $\tau = 0.030 \text{ sec}$ in NbBr_5 . The asymptotes shown by the broken lines correspond to the T^{-2} dependence of T_1^{-1} .

Table 2. Debye temperature θ and scaling time τ .

Compound	NbCl_5			NbBr_5		
	ax C, C'	eq B, B'	br A	ax CC'	eq BB'	br A, A'
$\theta(\text{K})$	146	146	146	94	94	94
$\tau(\text{sec})$	0.78	0.91	1.02	0.031	0.030	0.046

pound, the averaged values are given in Table 2. In the fitting the two parameters θ and τ are not independent of each other. However θ is determined in effect from the portion where $(T_1 T^2)^{-1}$ changes abruptly. Therefore θ is nearly independent of the detailed dependence at such low temperatures that (5) predicts for T_1^{-1} the power dependence of T^7 [3].

The obtained values of θ are reasonable as compared e.g. with the values 183 K for AgCl and 144 K for AgBr . The ratio $\theta(\text{NbBr}_5)/\theta(\text{NbCl}_5) = 0.64$ is close to the value 0.67 obtained from Lindemann's melting formula [15] with their melting points 481 K for NbCl_5 and 422 K for NbBr_5 . In (2), if ω_m is approximated by the lowest optical mode frequency, the

ratio is also consistent with the proportionality of θ to ω_m , because the ratio of the corresponding frequencies observed in these compounds range from 0.58 to 0.76 [16].

4.3 Estimation of Covalency

Now the value of λ can be estimated from the above determined τ . For halogen atoms the coupling constants in free atom, $e^2 Q q_{\text{at}}$, are determined with high accuracy by the atomic beam experiment [17], as given in Table 1. Since q_{at} , the expectation value of $(3z^2 - r^2)/r^5$ for the p_z state, is the product of the radial part $\langle r^{-3} \rangle_{\text{H}}$ and the angular part $\langle (3z^2 - r^2)/r^2 \rangle$ for p_z state, and since the latter is $4/5$, $e^2 Q \langle r^{-3} \rangle_{\text{H}}$ is given by $(5/4)e^2 Q q_{\text{at}}$. On the other hand, for the dependence of the covalency λ on the interionic distance r , Yosida and Moriya [4] assumed

$$\lambda \propto \exp(-r/\varrho) \quad (11)$$

for the following reason: Since λ is proportional to the square of the overlap integral, it is approximately proportional to the repulsive potential between ions, which itself is proportional to $\exp(-r/\varrho)$ according to Born and Mayer's theory. In their analysis of alkali halides an identical value of 0.345 \AA was employed for ϱ of all the halides. By substitution of these values into $N_{\mu\text{v}}$ in (3) and by the use in (9) of the crystal data given in Table 1 we obtain $61.3 \lambda^2$ for τ^{-1} of the C' line of NbCl_5 and $3070 \lambda^2$ for the CC' line in NbBr_5 . On equating these expressions to the values of τ^{-1} obtained from Table 2, we obtain the values of λ given in Table 3.

These values may be compared with those estimated from the NQR frequency. In [4], λ is defined as the amount of p electron which is transferred, in making covalent bonding, from the halogen ion to the metal ion and is supposed to produce the EFG with the largest component along the bond. Therefore, for terminal atoms, it should be compared with the number of p_z electron effective to the EFG, f , defined as [1]

$$f = \frac{e^2 Q q_{\text{mol}}}{e^2 Q q_{\text{at}}} \quad (12)$$

The $e^2 Q q_{\text{mol}}$ is related to the NQR frequency ν_Q by

$$\nu_Q = \frac{e^2 Q q_{\text{mol}}}{2h} (1 + \eta^2/3)^{1/2}, \quad (13)$$

where η denotes the asymmetry parameter. On the other hand, at the bridging atom the principal z -axis

Table 3. Two measures of covalency, λ and f .

Compound	NbCl_5			NbBr_5		
	ax	eq	br	ax	eq	br
λ	0.145	0.130	0.052	0.104	0.108	0.031
f	0.133	0.135	0.121	0.154	0.155	0.140

of the EFG is normal to the directions toward the two metal atoms due to the bond switching, as shown in Figure 3. Therefore f is given by half that calculated with (12). Using the values of ν_Q at 77 K with the assumption $\eta = 0$ and the value of $e^2 Q q_{\text{at}}$ in Table 1, we obtain the values of f in Table 3.

4.4 Comparison between λ and f

The agreement between λ and the corresponding f at terminal positions is fairly good, particularly in NbCl_5 , but some discrepancies are recognized. First, the λ 's for NbBr_5 are smaller than those for NbCl_5 , whereas the former f is larger than the latter one. Second, in NbCl_5 λ for the equatorial position is smaller than that for the axial one, whereas the former f is rather larger than the latter f . Third, the values of λ at the bridging positions are much smaller than the values of f in either compound.

The former two discrepancies are related to the use of the identical value for $-\lambda'/\lambda = 1/\varrho$. Indeed, in alkali halides the change of the halogen ion from fluorine through chlorine and bromine to iodine is associated with some increase of ϱ determined from the observed interionic distances and the compressibilities [18]. However, a more important effect may be that due to the π -character of the metal-halogen bond. In the above calculation σ -bond alone is assumed implicitly. However, the extraordinarily low NQR frequencies in the present compounds indicate that some degree of π -character is involved in the metal-halogen bond in addition to large ionicity [1]. By the following argument it is suggested that a larger value should then be used for ϱ : If $\lambda(r)$ is approximated by a linear function which vanishes at the ionic distance r_i and ϱ is determined as $-\lambda/(d\lambda/dr)$ at the covalent distance r_c , a relation $\varrho = r_i - r_c$ is obtained. Since r_c takes a smaller value for π -bond, ϱ takes a larger value. Since, according to an analysis of the NQR frequencies, the Nb-Br bond possesses larger π -character than the Nb-Cl [1], a larger degree of enlargement in ϱ , whence in λ from (3), is expected for the Nb-Br bond. This effect must

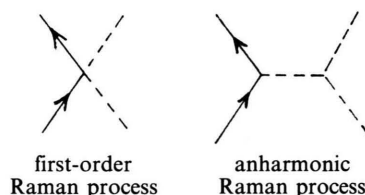
also be taken into consideration in comparison within the terminal positions in each compound. In the present dimeric structure, from consideration of the competition for d_e orbital in forming π -bond, a slightly larger π -character is expected for the equatorial atoms [1]. It is also expected from the ratio $a_{\text{eq}}/a_{\text{ax}} < 1$ for NbCl_5 in Table 1. Therefore a slightly larger value should be used for ρ of the equatorial atoms, and then a little larger value should result for λ . For the second discrepancy the neglect of η is also responsible. For the case of $I = 3/2$ the value can not be determined from measurement of the NQR frequencies alone, but it is expected to be larger at the equatorial nuclei than at the axial ones [1]. Thus, if this effect is corrected in (12) with (13), we will find somewhat smaller f for the equatorial atoms than in the table. In contrast to NbCl_5 , close values of λ are obtained for the axial and equatorial positions in NbBr_5 . The approaching unity of the ratio $\lambda_{\text{eq}}/\lambda_{\text{ax}}$ accompanying the variation from chloride to bromide corresponds to the approaching the octahedral symmetry of the structure [1]. Close amounts of π -character in the two bonds are also suggested by the close temperature coefficients of their NQR frequencies in Figure 1.

The third discrepancy is considered to be mainly due to the failure in equivalency of the halogen atoms. In fact, the isotropic temperature factor reported in X-ray analysis of NbCl_5 [5] is $3.1 \pm 0.1 \text{ \AA}^2$ for axial and $3.2 \pm 0.2 \text{ \AA}^2$ for equatorial atoms, whereas $1.7 \pm 0.6 \text{ \AA}^2$ for bridging ones, in an average within the positions. The neglect of this smaller mobility of the bridging atoms is considered to lead to such a serious underestimation of λ . At the same time it should raise the λ for terminal atoms, though the degree is not so large because of the larger number of terminal atoms involved in the crystal. The too small values of λ for the bridging atoms may be partly attributed to the departure of that bond from the cylindrical symmetry also assumed in the calculation [4].

4.5 Final Remarks

By these corrections the values of λ in Table 3 will be enlarged by factors of 1 to 2. Nevertheless, we can still say that the agreement between λ and f is rather good for this kind of calculation. The remaining discrepancy may be attributed to anharmonicity of the Raman process, which can not be distinguished from

the first-order Raman process by the temperature dependence (cf. [19], p. 2445).



In the present study the relaxation was examined by NQR in molecular crystals. One advantage of NQR over NMR is that, since the spin system is then quantized along the principal axis of the EFG at each nucleus, the averaging over orientation is not required, even if powder samples are used. An advantage of molecular crystals is that, in the calculation of $N_{\mu\nu}$ it is sufficient to take only a few bonds into account. This makes the results quite simple as compared with the case of ionic crystals. However, most important is that accurate information about the covalency can be obtained at the same time, because the NQR frequency in molecular crystals is directly related to it.

5. Conclusion

The halogen nuclear spin-lattice relaxation in HTM of NbCl_5 and NbBr_5 has been shown to originate from the quadrupolar interaction with lattice vibrations through the Raman process. It has been shown that a precise measurement of temperature dependence of T_1 serves as a powerful method for the determination of the Debye temperature. The wide difference of T_1 between NbCl_5 and NbBr_5 is attributed not only to the wide difference in the coupling constant but also to the differences in the Debye temperature as well as other quantities. The degree of covalency of the bonds between niobium and halogen atoms has been estimated, and the relaxation times of the halogen nuclei have been related to the NQR frequencies through the covalency.

The Raman process due to lattice vibrations exists also in other solids as the relaxation mechanism, provided the quadrupole moment is involved. The present study shows that the order of magnitude of the contribution can be correctly estimated by Yosida and Moriya's theory in some cases.

Appendix

According to [4], the transition probability from $I_z = m$ to $m + \mu$ due to the Raman process is given by

$$P(m, m + \mu) = \frac{A'^2 c^3 |Q_{\mu m}|^2}{2\pi^3 a^7 d^2 v^3} T^{*2} \sum_{\nu=1}^4 N_{\mu\nu} D_{\nu}(T^*), \quad (\text{A1})$$

where

$$A' = \frac{3}{5} e A \left\langle \frac{1}{r^3} \right\rangle_{\text{H}}, \quad A = \frac{e Q}{2I(2I-1)}, \quad (\text{A2})$$

$$Q_{\mu m} = \langle m + \mu | Q_{\mu} | m \rangle \quad \text{with} \quad \begin{aligned} Q_{\pm 1} &= \frac{1}{2} (I_z I_{\pm} + I_{\pm} I_z) \\ Q_{\pm 2} &= I_{\pm}^2. \end{aligned} \quad (\text{A3})$$

For a system of $I = 3/2$ with $\pm m$ degeneracy, T_1^{-1} is given by $2\{P(1/2, 3/2) + P(-1/2, 3/2)\}$. Using $|Q_{2, -1/2}|^2 = 4|Q_{1, 1/2}|^2 = 12$, we obtain the expression (1) in the text.

The expression of $N_{\mu\nu}$ for any structure is given by (4.28) with (4.35) and (4.36) of [4]. In (4.28) summation is made about the unit vectors \mathbf{n} and \mathbf{n}' from the halogen atom to the metal atoms. For the present case, where terminal atoms are bonded to one metal atom, it is sufficient to take into account only one vector corresponding to that bond. Then, for their direction cosines α, β , and γ in the principal axis system taken as in Fig. 3, we have $\alpha(\mathbf{n}) = \alpha(\mathbf{n}') = 0$, $\beta(\mathbf{n}) = \beta(\mathbf{n}') = 0$ and $\gamma(\mathbf{n}) = \gamma(\mathbf{n}') = 1$. On the other hand, since the bridging atom is bonded to two niobium atoms I and II, the summation must be taken over two vectors directed toward them, \mathbf{n}_I and \mathbf{n}_{II} . For their direction cosines we have $\alpha(\mathbf{n}_I) = \alpha(\mathbf{n}_{II}) = \cos(\phi/2)$, $\beta(\mathbf{n}_I) = -\beta(\mathbf{n}_{II}) = \sin(\phi/2)$, $\gamma(\mathbf{n}_I) = \gamma(\mathbf{n}_{II}) = 0$. By substitution of these relations and use of (4.11') of [4] we obtain the expression for $N_{\mu\nu}$ in the text.

The expressions for L_{ν} are derived by averaging $B_{\mathbf{n}\sigma} B_{\mathbf{n}\sigma'}, B_{\mathbf{n}'\sigma} B_{\mathbf{n}'\sigma'}$ in (4.26') of [4] about the directions of \mathbf{k} and \mathbf{k}' for the case of the vectors \mathbf{n} and \mathbf{n}' making a general angle ϕ .

- [1] N. Okubo, J. Phys. Soc. Japan **51**, 524 (1982) and the references found therein.
- [2] N. Okubo, H. Matsuura, and Y. Abe, J. Phys. Soc. Japan **59**, 2289 (1990).
- [3] J. Van Kranendonk, Physica **XX**, 781 (1954).
- [4] K. Yosida and T. Moriya, J. Phys. Soc. Japan **11**, 33 (1956).
- [5] A. Zalkin and D. E. Sands, Acta Crystallogr. **11**, 615 (1958).
- [6] K. M. Alexander and F. Fairbrother, J. Chem. Soc. **1949**, S223.
- [7] R. F. Rolsten, J. Phys. Chem. **62**, 126 (1958).
- [8] N. Okubo and Y. Abe, Phys. Lett. **A 73**, 247 (1979).
- [9] N. Okubo and Y. Abe, J. Phys. Soc. Japan **51**, 1347 (1982).
- [10] N. Okubo and Y. Abe, Phys. Lett. **A 106**, 435 (1984).
- [11] H. Sekiya, N. Okubo, and Y. Abe, Phys. Lett. **A 152**, 495 (1991).
- [12] D. E. Woesner and H. S. Gutowsky, J. Chem. Phys. **39**, 440 (1963).
- [13] K. R. Jeffrey and R. L. Armstrong, Can. J. Phys. **44**, 2315 (1966).
- [14] L. Pauling, The Nature of Chemical Bond, Cornell University Press, Ithaca 1960, 3rd ed.
- [15] J. M. Ziman, Principles of the Theory of Solids, Cambridge University Press, Cambridge 1965.
- [16] I. R. Beattie *et al.*, J. Chem. Soc. A **1968**, 2765.
- [17] T. P. Das and E. L. Hahn, Nuclear Quadrupole Resonance Spectroscopy, Solid State Physics, F. Seitz and D. Turnbull, Academic Press, New York 1958.
- [18] M. Born and K. Huang, Dynamical Theory of Crystal Lattices, Clarendon Press, Oxford 1954.
- [19] J. Van Kranendonk and M. B. Walker, Canad. J. Phys. **46**, 2441 (1968).